Check for updates

Age- and Sex-Specific Changes in CMR Feature Tracking-Based Right Atrial and Ventricular Functional Parameters in Healthy Asians

Shuang Leng [1†], Jiajun Guo [2†], Ru-San Tan [1,3], Ping Chai [4,5], Lynette Teo [5,6], Marielle V. Fortier [3,7,8], Chao Gong [2], Xiaodan Zhao [1], Ching Ching Ong [5,6], John C. Allen [3], Wen Ruan [1,3], Angela S. Koh [1,3], Teng Hong Tan [3,7], James W. Yip [4,5], Ju Le Tan [1,3], Yucheng Chen [2*] and Liang Zhong [1,3*]

[1] National Heart Centre Singapore, Singapore, Singapore, [2] Cardiology Division, Department of Medicine, West China Hospital, Sichuan University, Chengdu, China, [3] Duke-NUS Medical School, Singapore, Singapore, [4] Department of Cardiology, National University Heart Centre, Singapore, Singapore, [5] Yong Loo Lin School of Medicine, National University of Singapore, Singapore, Singapore, [6] Department of Diagnostic Imaging, National University Hospital, Singapore, Singapore, [7] KK Women's and Children's Hospital, Singapore, Singapore, [8] Singapore Institute for Clinical Sciences, A*STAR, Singapore, Singapore

Cardiovascular magnetic resonance (CMR) is the reference standard for non-invasive assessment of right-sided heart function. Recent advances in CMR post-processing facilitate quantification of tricuspid annular (TA) dynamics and longitudinal strains of the right ventricle (RV) and right atrium (RA). We aimed to determine age- and sex-specific changes in CMR-derived TA dynamics, and RV and RA functional parameters in healthy Asian adults. We studied 360 healthy subjects aged 21–79 years, with 30 men and 30 women in each of the six age groups. Functional parameters of RV and RA were measured on standard four-chamber cine CMR using fast feature tracking: (1) TA peak velocities (systolic velocity S′, early diastolic velocity E′, late diastolic velocity A′) and TA plane systolic excursion (TAPSE); (2) RV global longitudinal strain (GLS) and strain rates; and (3) RA phasic longitudinal strains and strain rates. S′ and TAPSE exhibited negative correlations with age. RV GLS was significantly higher in females than in males but not associated with age in both sexes. Females had similar E′, lower A′, and higher E′/A′ ratios compared to males. Positive associations of E′ and E′/A′, and negative association of A′ with age were observed in both sexes. Females had higher RA reservoir and conduit strains compared to males. There were significantly negative and positive associations between RA conduit and booster strains, respectively, with age. Age- and sex-specific reference ranges were established, and associations revealed, for fast CMR feature tracking parameters of right heart function in a large normal Asian population.

Keywords: cardiovascular magnetic resonance, feature tracking, right ventricular function, right atrial function, age, sex

INTRODUCTION

The right side of the heart has traditionally received less attention than the left, yet there is a growing body of evidence showing that right heart size and function are perhaps of equal importance in providing diagnostic and prognostic information in a wide range of cardiovascular diseases (1).

Cardiovascular magnetic resonance (CMR) imaging is the current gold standard for quantitation of right ventricular (RV) geometry and function (2). Guidelines recommend CMR for assessment of global RV functional parameters such as RV volumes, ejection fraction (EF), and cardiac output (3). Recent advances in CMR post-processing have facilitated reliable quantitation of tricuspid annular (TA) dynamics and longitudinal strains of the RV and right atrium (RA) using feature tracking (4–8). CMR-based TA systolic velocity (S′), early diastolic velocity (E′), late diastolic velocity (A′), and TA plane systolic excursion (TAPSE) have been reported to be significantly lower in patients diagnosed with heart failure (4), hypertrophic cardiomyopathy (4), repaired tetralogy of Fallot (rTOF) (4, 5), unrepaired atrial septal defect (5), and severe tricuspid insufficiency (6) than in normal controls. RV and RA longitudinal strains can be quantified either by feature tracking of the whole RV and RA endocardium, respectively (9, 10), or more rapidly by tracking discrete anatomical points on standard cine CMR (7, 8). A prior study demonstrated the prognostic utility of impaired fast CMR feature tracking-derived RA strain parameters for predicting clinical and hemodynamic deterioration in patients with pulmonary arterial hypertension (PAH) (7). The quantitative RV fast strain and strain rate parameters assessed from CMR identify abnormalities of RV function in rTOF and PAH and are predictive of exercise capacity, RV decompensation, and clinical risks in these patients (8).

The emerging importance of these parameters motivates efforts to define normal ranges and distributions in a healthy population. In addition, most CMR normal ranges for right heart size and volume have been established for Caucasians and may not be generalizable to other ethnicities (11). Accordingly, the aim of this study is to determine age- and sex-specific changes in CMR-derived RV and RA dimensions and functional (systolic and diastolic) parameters among healthy Asian subjects.

Abbreviations: A′, peak tricuspid annular late diastolic velocity; BSA, body surface area; CMR, cardiovascular magnetic resonance; ε_a, right atrial booster strain; ε_e, right atrial conduit strain; ε_s, right atrial reservoir strain; E′, peak tricuspid annular early diastolic velocity; EDV, end-diastolic volume; EF, ejection fraction; ESV, end-systolic volume; GLS, global longitudinal strain; GLSR$_a$, global longitudinal strain rate during late diastole, GLSR$_e$, global longitudinal strain rate during early diastole; GLSR$_s$, global longitudinal strain rate during systole; LV, left ventricle; PAH, pulmonary arterial hypertension; RA, right atrium; rTOF, repaired tetralogy of Fallot; RV, right ventricle; S′, peak tricuspid annular systolic velocity; SD, standard deviation; SR$_a$, right atrial booster strain rate; SR$_e$, right atrial conduit strain rate; SR$_s$, right atrial reservoir strain rate; SV, stroke volume; TA, tricuspid annular; TAPSE, tricuspid annular plane systolic excursion; TDI, tissue Doppler imaging.

MATERIALS AND METHODS

Study Population

In this multicenter study, 360 subjects (aged 21–79 years, 180 males and 180 females) without known cardiovascular disease were enrolled from three hospitals between 2014 and 2019. The subjects were recruited from the (1) Cardiac Aging study (12), (2) INITIATE study, and (3) Database of healthy controls in West China Hospital. All subjects (1) had no known cardiovascular disease and demonstrated no signs of cardiovascular disease in prior electrocardiographic or echocardiographic investigations, (2) displayed no uncontrolled cardiovascular risk factors at the time of enrollment (systolic blood pressure ≤140 mmHg and diastolic blood pressure ≤90 mmHg without anti-hypertensive treatment, total cholesterol <6.2 mmol/L, fasting glucose <7 mmol/L, body mass index <30 kg/m^2, and current non-smoker status), and (3) had no significant kidney or lung disease. Other exclusion criteria were cerebrovascular disease or nervous system disease, cancer, autoimmune diseases, recent systemic infection (within a month), recent surgery or severe trauma (within a month), any recent medications, and a history of implantation of a pacemaker or other metals that are contraindicated for CMR. The institutional review board of each hospital approved the study protocol. Informed consent was obtained from each participant.

CMR Acquisition

CMR acquisitions were performed using a 3T magnetic resonance scanner (Ingenia, Philips Healthcare, The Netherlands) at National Heart Centre Singapore, a 1.5T MAGNETOM Aera magnetic resonance scanner (Siemens Healthineers, Erlangen, Germany) at National University Hospital Singapore, and a 3T MAGNETOM Tim Trio magnetic resonance scanner (Siemens Healthineers, Erlangen, Germany) at West China Hospital (Sichuan China). End-expiratory breath-hold-balanced steady-state free precession cine images were acquired in standard short- and long-axis views. Typical parameters for the Philips scanner were as follows: repetition time (TR)/echo time (TE), 3/1 ms; matrix, 240 × 240; flip angle, 45°; field of view, 300 × 300 mm; pixel spacing, 1.25 × 1.25 mm; slice thickness, 8 mm; number of frames, 30/40 per cardiac cycle. Parameters for the 1.5T Siemens scanner were: TR/TE, 33/1 ms; matrix, 192 × 180; flip angle, 58°; field of view, 320×300 mm; pixel spacing, 1.67 × 1.67 mm; slice thickness, 6 mm; number of frames, 30 per cardiac cycle. Parameters for the 3T Siemens scanner were: TR/TE, 3.4/1.3 ms; matrix, 192 × 162; flip angle, 50°; field of view, 320 × 270 mm; pixel spacing, 1.67 × 1.67 mm; slice thickness, 8 mm; and number of frames, 25 per cardiac cycle.

Echocardiography

A sub-study was conducted to validate CMR-derived TA dynamics against those measured using echocardiography. Echocardiography was performed on the same day as CMR using a commercial ultrasound system (Aloka α10, Japan). TA velocities and displacement were measured using tissue Doppler
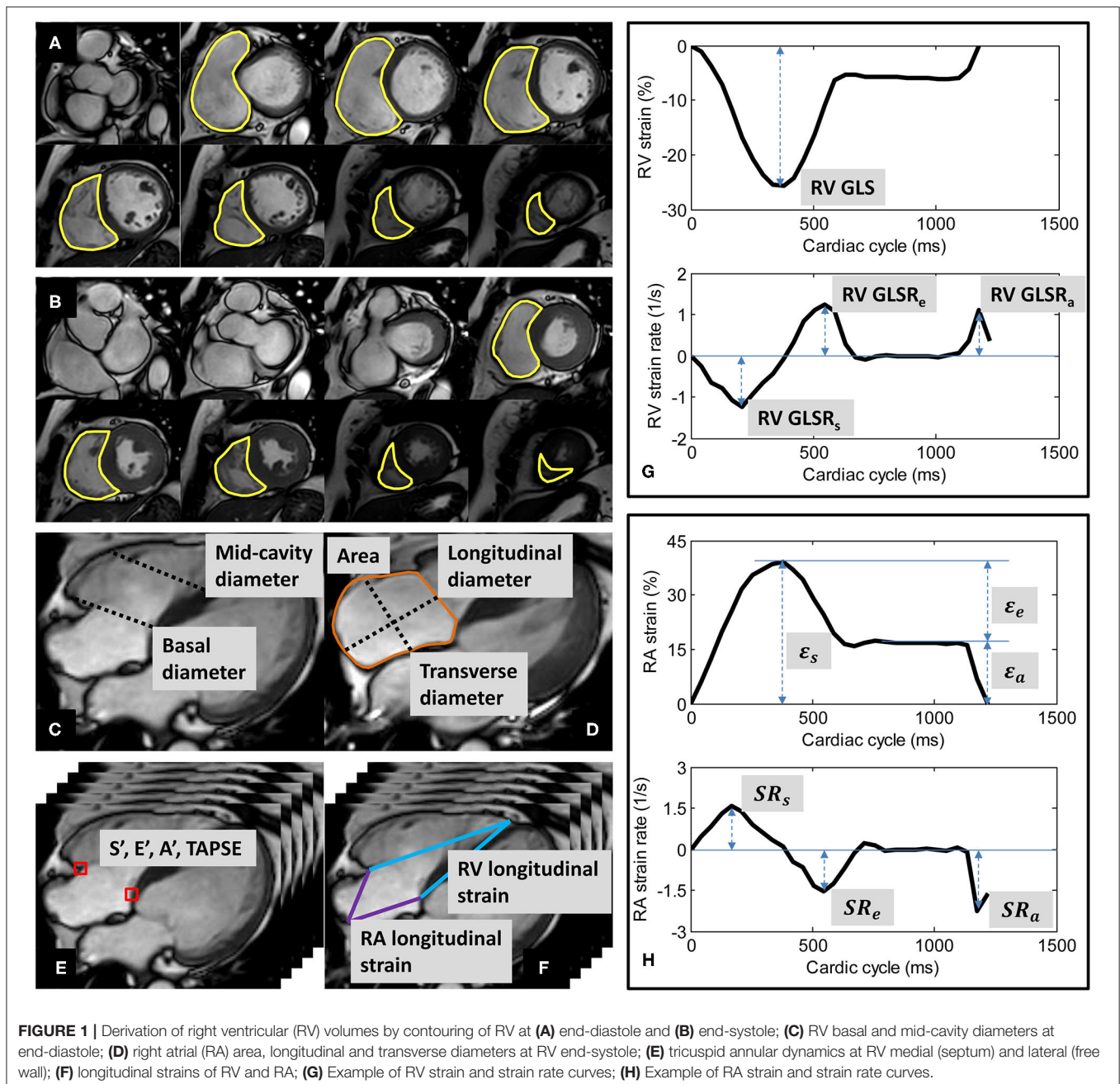
imaging (TDI) and M-mode, respectively, in the apical four-chamber view.

CMR Data Analysis

The parameters measured were (1) RV volumes and RVEF (derived from standard CMR volumetric analysis), (2) Two-dimensional chamber dimensions (RV chamber diameters and RA area and diameters), (3) TA velocities (systolic velocity S', early diastolic velocity E', and late diastolic velocity A') and displacement (TAPSE), (4) RV longitudinal strain and strain rates, and (5) RA phasic (reservoir, conduit, and booster) longitudinal strains and strain rates.

Volumetric Analysis and Chamber Dimensions

Endocardial contours were manually traced from the stack of short-axis cine images to obtain RV end-diastolic volume (EDV) and end-systolic volume (ESV), from which stroke volume (SV) and EF were derived (**Figures 1A,B**). Papillary muscles and trabeculae were included in the blood volume (3). RV size was measured from the four-chamber view at end-diastole. RV basal diameter was measured at the level of the tricuspid valve, and mid-cavity diameter was measured in the middle third of the RV at the level of the left ventricular (LV) papillary muscle (13) (**Figure 1C**).

FIGURE 1 | Derivation of right ventricular (RV) volumes by contouring of RV at **(A)** end-diastole and **(B)** end-systole; **(C)** RV basal and mid-cavity diameters at end-diastole; **(D)** right atrial (RA) area, longitudinal and transverse diameters at RV end-systole; **(E)** tricuspid annular dynamics at RV medial (septum) and lateral (free wall); **(F)** longitudinal strains of RV and RA; **(G)** Example of RV strain and strain rate curves; **(H)** Example of RA strain and strain rate curves.

RA area and diameters were measured from the four-chamber view at RV end-systole. RA longitudinal diameter was measured as the distance between the midpoint of the line joining the medial and lateral (free wall) insertions of the tricuspid valve and the posterior wall (roof) of the RA. RA transverse diameter was measured as the orthogonal line bisecting the longitudinal diameter (14) (**Figure 1D**).

All chamber dimension measurements were reported as both absolute values and indexed values normalized to body surface area (BSA).

Tricuspid Annular Velocities and Displacement

Custom software developed in the MATLAB environment (MathWorks Inc., MA, USA) and validated in prior studies (4, 7, 8, 15–19) was used to perform the semi-automatic tracking of medial and lateral tricuspid valve insertions in the four-chamber view (**Figure 1E**). A video of the TA tracking and resultant TA velocity and displacement curves are shown in **Supplementary Materials**. Peak TA velocities were read off the velocity curve during systole (S′), early diastole (E′), late diastole (A′); TAPSE—TA displacement at end-systole—was read off the displacement curve (4, 7). We reported mean values for S′, E′, A′, and TAPSE averaged from medial and lateral TA measurements.

Longitudinal Strains of RV and RA

Using the same custom software, the RV epicardial apex and the RA roof point were tracked in the four-chamber view over the cardiac cycle (**Figure 1F**). We followed the convention of determining RV apex location by its proximity to the LV apex. The RV apex is close to but separated from the LV apex by the interventricular septal wall, which can be seen on the four-chamber view (13). The RA roof was localized to the intersection of the RA posterior wall and the RA longitudinal diameter.

The distance (L) from either the medial or the lateral tricuspid valve insertion to the RV epicardial apex on the four-chamber view was measured at any time point (t). RV strain value at time t with respect to RV end-diastole (time 0) was calculated using the formula for Lagrangian strain: $(L(t) - L(0)) \times 100/L(0)$ (8). RV global longitudinal strain (GLS)—strain value at end-systole— was read off the strain curve, and peak global longitudinal strain rates at RV systole ($GLSR_s$), early diastole ($GLSR_e$), and late diastole ($GLSR_a$) were calculated as first time-derivatives of the strain curve at the corresponding cardiac phases (8) (**Figure 1G**).

Similarly, RA longitudinal strain (ε) was derived from the time-varying distances between either the medial or the lateral tricuspid valve insertion and the RA roof point (7). RA reservoir strain (ε_s), conduit strain (ε_e) and booster strain (ε_a) were read off the generated strain curve at RV end-systole, diastasis, and pre-RA systole, respectively, and the corresponding peak strain rates (SR_s, SR_e, and SR_a) calculated as first time-derivatives of the strain curve at the corresponding cardiac phases (7) (**Figure 1H**).

A video showing the derivation of RV and RA strain is given in **Supplementary Materials**. Mean RV and RA strain and strain rate parameters averaged from medial and lateral TA measurements were used for all analyses. RV strain and strain rate parameters were presented as absolute values.

Conventional Feature Tracking Strain

A sub-study was conducted to validate the fast feature tracking-derived RA and RV strain measurements against those derived from conventional CMR RA and RV endocardial feature tracking using dedicated QStrain software (Version 2.0, Medis BV, Leiden, The Netherlands).

Statistical Analysis

The distribution normality of continuous variables was assessed using the Shapiro-Wilk test. Data were expressed as mean ± standard deviation (SD), and reported across six pre-specified age groups stratified by sex. Age-specific reference limits were defined as mean ± 1.96·SD. Values obtained in females and males were compared using Student's t-test. For either sex,

TABLE 1 | Demographics and right heart function parameters of the control population.

Parameters	Total (n = 360)	Men (n = 180)	Women (n = 180)	P-value
Demographics				
Age (years)	50 ± 17	51 ± 17	49 ± 17	0.464
Height (cm)	163 ± 9	169 ± 7	158 ± 6	<0.0001
Weight (kg)	61 ± 11	66 ± 10	56 ± 9	<0.0001
BSA (m²)	1.7 ± 0.2	1.8 ± 0.2	1.6 ± 0.2	<0.0001
BMI (kg/m²)	22.8 ± 2.8	23.3 ± 2.7	22.4 ± 2.8	0.002
Systolic blood pressure (mmHg)	124 ± 12	127 ± 10	120 ± 12	<0.0001
Diastolic blood pressure (mmHg)	76 ± 9	78 ± 7	74 ± 10	<0.0001
Heart rate (beats per minute)	74 ± 11	74 ± 12	73 ± 11	0.881
Right ventricular function (systolic and diastolic)				
RVEF (%)	58 ± 7	57 ± 7	60 ± 7	0.001
S′ (cm/s)	9.5 ± 1.4	9.6 ± 1.6	9.4 ± 1.2	0.070
E′ (cm/s)	10.5 ± 2.9	10.3 ± 3.0	10.8 ± 2.9	0.138
A′ (cm/s)	10.9 ± 2.3	11.2 ± 2.2	10.5 ± 2.4	0.004
E′/A′	1.0 ± 0.4	1.0 ± 0.4	1.1 ± 0.5	0.001
TAPSE (mm)	19.5 ± 2.6	19.3 ± 2.6	19.7 ± 2.5	0.118
RV GLS (%)	24 ± 4	23 ± 3	26 ± 3	<0.0001
RV GLSR$_s$ (1/s)	1.3 ± 0.3	1.3 ± 0.3	1.3 ± 0.2	0.052
RV GLSR$_e$ (1/s)	1.5 ± 0.4	1.3 ± 0.4	1.6 ± 0.5	<0.0001
RV GLSR$_a$ (1/s)	1.2 ± 0.4	1.2 ± 0.4	1.2 ± 0.4	0.703
Right atrial phasic function				
Reservoir strain ε_s (%)	46 ± 9	43 ± 8	48 ± 9	<0.0001
Conduit strain ε_e (%)	24 ± 8	22 ± 7	26 ± 9	<0.0001
Booster strain ε_a (%)	22 ± 5	21 ± 5	22 ± 6	0.408
Reservoir strain rate SR_s (1/s)	2.4 ± 0.5	2.3 ± 0.5	2.4 ± 0.5	0.019
Conduit strain rate SR_e (1/s)	−2.2 ± 0.8	−2.0 ± 0.7	−2.3 ± 0.8	0.001
Booster strain rate SR_a (1/s)	−2.7 ± 0.7	−2.7 ± 0.6	−2.8 ± 0.7	0.147

Data are presented as mean ± SD. P-value is for t-test between sexes. BSA, body surface area; BMI, body mass index; RV, right ventricular; EF, ejection fraction; S', peak systolic tricuspid annular velocity; E', peak early diastolic tricuspid annular velocity; A', peak late diastolic tricuspid annular velocity; TAPSE, tricuspid annular plane systolic excursion; GLS, global longitudinal strain; GLSR$_s$, peak systolic global longitudinal strain rate; GLSR$_e$, peak early diastolic global longitudinal strain rate; GLSR$_a$, peak late diastolic global longitudinal strain rate.

linear regression was used to characterize the relationship of right heart measurements with age. Intra- and inter-observer variability of study parameters was studied in a selected subgroup of 20 cases using Bland-Altman analysis and coefficient of variation. Statistical analyses were performed using SPSS software (Version 17.0, IBM, Chicago, IL, USA). $P \leq 0.05$ indicated statistical significance.

RESULTS

Baseline Characteristics and Summary Results

We recruited 360 healthy individuals (male:female 180:180, age range 21–79 years). Baseline demographics and right heart CMR measurements stratified by sex are given in **Table 1**. Age group-specific CMR measurements stratified by sex are presented in **Tables 2**, **3**. **Figures 2**, **3** show RV volume and systolic and diastolic RV function parameters plotted against age with 5th, 50th, and 95th percentile values in males and females, respectively. **Figures 4**, **5** show RA dimensions and phasic function parameters vs. age with 5th, 50th, and 95th percentile values in males and females, respectively. Measurements of right heart dimensions and volumes stratified by sex and age group are presented in **Supplementary Tables 1–3**.

Validation of Fast CMR Feature Tracking-Derived Measurements

Results from a sub-study of 60 subjects comprising 10 randomly selected from each of the six age groups showed that fast CMR feature tracking-derived TA dynamic measurements, RA and RV strain measurements were in good agreement with echocardiographic ($r = 0.76$–0.83,

TABLE 2 | Males: right heart function parameters by age group [mean ± SD (reference range, lower/upper limits calculated as mean ± 1.96·SD)].

Parameters	<30 (n = 30)	30–39 (n = 30)	40–49 (n = 30)	50–59 (n = 30)	60–69 (n = 30)	≥70 (n = 30)
Right ventricular function (systolic and diastolic)						
RVEF (%)	55 ± 7 (42, 68)	55 ± 7 (43, 68)	55 ± 6 (44, 66)	58 ± 7 (44, 71)	58 ± 7 (45, 71)	62 ± 7 (48, 76)
S′ (cm/s)	10.6 ± 1.7 (7.4, 13.9)	9.9 ± 1.2 (7.5, 12.4)	9.7 ± 1.4 (7.0, 12.4)	9.5 ± 1.5 (6.7, 12.4)	9.2 ± 1.6 (6.1, 12.3)	8.9 ± 1.5 (5.9, 11.9)
E′ (cm/s)	14.2 ± 2.6 (9.1, 19.2)	12.3 ± 1.9 (8.6, 16.0)	10.6 ± 2.1 (6.6, 14.7)	9.2 ± 1.6 (6.0, 12.3)	8.6 ± 1.7 (5.2, 11.9)	7.7 ± 1.7 (4.3, 11.0)
A′ (cm/s)	9.8 ± 1.7 (6.5, 13.0)	10.2 ± 1.6 (7.0, 13.4)	10.7 ± 1.8 (7.2, 14.3)	11.2 ± 1.7 (8.0, 14.5)	12.1 ± 2.3 (7.6, 16.6)	12.9 ± 1.9 (9.1, 16.8)
E′/A′	1.4 ± 0.3 (0.9, 1.9)	1.2 ± 0.2 (0.8, 1.7)	1.0 ± 0.3 (0.5, 1.5)	0.8 ± 0.2 (0.5, 1.1)	0.7 ± 0.2 (0.4, 1.0)	0.6 ± 0.1 (0.3, 0.9)
TAPSE (mm)	20.4 ± 2.8 (15.0, 25.8)	19.7 ± 2.3 (15.1, 24.2)	19.5 ± 2.5 (14.6, 24.4)	19.1 ± 2.4 (14.5, 23.8)	18.9 ± 2.4 (14.2, 23.6)	18.1 ± 2.8 (12.5, 23.6)
RV GLS (%)	23 ± 3 (18, 28)	23 ± 3 (17, 28)	22 ± 3 (16, 29)	23 ± 3 (17, 30)	23 ± 3 (17, 30)	24 ± 3 (17, 31)
RV GLSR$_s$ (1/s)	1.3 ± 0.2 (0.9, 1.7)	1.2 ± 0.2 (0.8, 1.6)	1.3 ± 0.3 (0.7, 1.8)	1.3 ± 0.3 (0.7, 1.8)	1.2 ± 0.3 (0.7, 1.8)	1.3 ± 0.3 (0.7, 1.9)
RV GLSR$_e$ (1/s)	1.7 ± 0.3 (1.1, 2.4)	1.6 ± 0.3 (1.1, 2.1)	1.3 ± 0.3 (0.8, 2.0)	1.2 ± 0.3 (0.7, 1.8)	1.1 ± 0.3 (0.4, 1.8)	1.1 ± 0.2 (0.6, 1.6)
RV GLSR$_a$ (1/s)	0.9 ± 0.2 (0.5, 1.3)	1.1 ± 0.3 (0.5, 1.6)	1.2 ± 0.3 (0.5, 1.8)	1.2 ± 0.2 (0.7, 1.7)	1.4 ± 0.4 (0.7, 2.1)	1.6 ± 0.3 (1.0, 2.1)
Right atrial phasic function						
Reservoir strain ε_s (%)	48 ± 9 (30, 66)	45 ± 8 (30, 61)	43 ± 8 (27, 58)	41 ± 8 (26, 57)	42 ± 8 (27, 58)	41 ± 8 (26, 57)
Conduit strain ε_e (%)	30 ± 8 (14, 47)	27 ± 5 (18, 36)	22 ± 6 (10, 34)	20 ± 5 (9, 30)	18 ± 5 (8, 28)	18 ± 4 (10, 26)
Booster strain ε_a (%)	18 ± 3 (11, 24)	19 ± 4 (10, 27)	20 ± 4 (13, 28)	22 ± 4 (14, 30)	24 ± 6 (13, 36)	24 ± 6 (12, 36)
Reservoir strain rate SR_s (1/s)	2.5 ± 0.5 (1.5, 3.4)	2.4 ± 0.5 (1.5, 3.3)	2.2 ± 0.5 (1.3, 3.2)	2.2 ± 0.5 (1.2, 3.1)	2.2 ± 0.5 (1.1, 3.3)	2.3 ± 0.6 (1.2, 3.4)
Conduit strain rate SR_e (1/s)	−2.9 ± 0.7 (−4.2, −1.6)	−2.5 ± 0.5 (−3.4, −1.6)	−2.0 ± 0.5 (−3.1, −1.0)	−1.7 ± 0.4 (−2.6, −0.9)	−1.6 ± 0.4 (−2.4, −0.7)	−1.5 ± 0.4 (−2.3, −0.7)
Booster strain rate SR_a (1/s)	−2.4 ± 0.6 (−3.5, −1.3)	−2.3 ± 0.5 (−3.3, −1.3)	−2.5 ± 0.4 (−3.3, −1.7)	−2.6 ± 0.6 (−3.7, −1.5)	−2.9 ± 0.7 (−4.4, −1.5)	−3.1 ± 0.7 (−4.4, −1.8)

RV, right ventricular; EF, ejection fraction; S′, peak systolic tricuspid annular velocity; E′, peak early diastolic tricuspid annular velocity; A′, peak late diastolic tricuspid annular velocity; TAPSE, tricuspid annular plane systolic excursion; GLS, global longitudinal strain; GLSR$_s$, peak systolic global longitudinal strain rate; GLSR$_e$, peak early diastolic global longitudinal strain rate; GLSR$_a$, peak late diastolic global longitudinal strain rate.

TABLE 3 | Females: right heart function parameters by age group [mean ± SD (reference range, lower/upper limits calculated as mean ± 1.96·SD)].

Parameters	<30 (n = 30)	30–39 (n = 30)	40–49 (n = 30)	50–59 (n = 30)	60–69 (n = 30)	≥70 (n = 30)
Right ventricular function (systolic and diastolic)						
RVEF (%)	58 ± 5 (48, 68)	58 ± 8 (43, 73)	58 ± 7 (43, 72)	58 ± 6 (46, 70)	62 ± 6 (50, 74)	63 ± 7 (50, 77)
S′ (cm/s)	10.0 ± 1.2 (7.7, 12.4)	9.6 ± 1.2 (7.2, 11.9)	9.5 ± 1.3 (7.0, 12.0)	9.2 ± 1.3 (6.7, 11.7)	9.0 ± 1.1 (6.9, 11.2)	8.8 ± 1.0 (6.9, 10.8)
E′ (cm/s)	14.5 ± 2.2 (10.2, 18.7)	12.1 ± 1.7 (8.6, 15.5)	11.5 ± 1.9 (7.7, 15.3)	10.5 ± 2.1 (6.4, 14.7)	8.7 ± 1.9 (4.9, 12.5)	7.5 ± 1.5 (4.7, 10.4)
A′ (cm/s)	8.5 ± 1.7 (5.1, 11.9)	9.6 ± 1.8 (6.0, 13.1)	10.2 ± 1.9 (6.4, 14.0)	11.1 ± 2.0 (7.2, 14.9)	11.5 ± 2.4 (6.7, 16.2)	12.3 ± 2.3 (7.8, 16.8)
E′/A′	1.7 ± 0.4 (1.0, 2.5)	1.3 ± 0.3 (0.7, 1.9)	1.2 ± 0.3 (0.6, 1.7)	1.0 ± 0.2 (0.5, 1.4)	0.8 ± 0.2 (0.4, 1.2)	0.6 ± 0.2 (0.3, 1.0)
TAPSE (mm)	20.8 ± 2.4 (16.0, 25.6)	20.1 ± 2.5 (15.2, 25.0)	20.2 ± 2.4 (15.4, 25.0)	19.7 ± 2.5 (14.8, 24.5)	19.3 ± 2.3 (14.8, 23.7)	18.0 ± 2.5 (13.2, 22.8)
RV GLS (%)	25 ± 3 (19, 32)	26 ± 3 (19, 33)	26 ± 4 (18, 34)	25 ± 3 (18, 32)	26 ± 3 (19, 32)	27 ± 4 (20, 34)
RV GLSR$_s$ (1/s)	1.3 ± 0.2 (0.9, 1.7)	1.3 ± 0.2 (0.9, 1.7)	1.3 ± 0.3 (0.8, 1.8)	1.3 ± 0.2 (0.9, 1.8)	1.3 ± 0.3 (0.8, 1.9)	1.4 ± 0.3 (0.7, 2.0)
RV GLSR$_e$ (1/s)	2.1 ± 0.4 (1.3, 2.8)	1.7 ± 0.3 (1.1, 2.3)	1.6 ± 0.4 (0.9, 2.4)	1.5 ± 0.5 (0.6, 2.4)	1.3 ± 0.5 (0.4, 2.2)	1.2 ± 0.3 (0.6, 1.8)
RV GLSR$_a$ (1/s)	0.9 ± 0.2 (0.5, 1.3)	1.1 ± 0.3 (0.5, 1.7)	1.2 ± 0.3 (0.6, 1.8)	1.3 ± 0.3 (0.8, 1.8)	1.3 ± 0.4 (0.6, 2.1)	1.7 ± 0.4 (0.9, 2.4)
Right atrial phasic function						
Reservoir strain ε_s (%)	56 ± 8 (40, 73)	49 ± 7 (36, 63)	49 ± 9 (33, 66)	44 ± 9 (26, 62)	45 ± 10 (25, 65)	44 ± 7 (29, 58)
Conduit strain ε_e (%)	39 ± 6 (26, 51)	30 ± 6 (17, 43)	28 ± 6 (17, 39)	23 ± 6 (11, 35)	20 ± 7 (6, 35)	18 ± 5 (8, 29)
Booster strain ε_a (%)	18 ± 4 (9, 26)	19 ± 4 (10, 26)	22 ± 5 (12, 31)	21 ± 5 (11, 31)	25 ± 5 (15, 36)	25 ± 5 (16, 35)
Reservoir strain rate SR_s (1/s)	2.8 ± 0.6 (1.5, 4.0)	2.4 ± 0.5 (1.5, 3.3)	2.4 ± 0.5 (1.5, 3.4)	2.2 ± 0.4 (1.5, 3.0)	2.4 ± 0.5 (1.3, 3.4)	2.4 ± 0.4 (1.6, 3.2)
Conduit strain rate SR_e (1/s)	−3.4 ± 0.7 (−4.7, −2.1)	−2.6 ± 0.5 (−3.7, −1.6)	−2.5 ± 0.5 (−3.5, −1.5)	−2.1 ± 0.5 (−3.2, −1.0)	−1.7 ± 0.5 (−2.7, −0.7)	−1.5 ± 0.4 (−2.3, −0.8)
Booster strain rate SR_a (1/s)	−2.5 ± 0.5 (−3.5, −1.4)	−2.5 ± 0.7 (−3.8, −1.2)	−2.8 ± 0.6 (−3.9, −1.6)	−2.8 ± 0.7 (−4.2, −1.3)	−3.0 ± 0.9 (−4.7, −1.2)	−3.1 ± 0.7 (−4.5, −1.8)

RV, right ventricular; EF, ejection fraction; S′, peak systolic tricuspid annular velocity; E′, peak early diastolic tricuspid annular velocity; A′, peak late diastolic tricuspid annular velocity; TAPSE, tricuspid annular plane systolic excursion; GLS, global longitudinal strain; GLSR$_s$, peak systolic global longitudinal strain rate; GLSR$_e$, peak early diastolic global longitudinal strain rate; GLSR$_a$, peak late diastolic global longitudinal strain rate.

$P < 0.0001$, **Supplementary Figure 1**) and conventional CMR endocardial tracking-derived results ($r = 0.75$–0.94, $P < 0.0001$, **Supplementary Figures 2–4**).
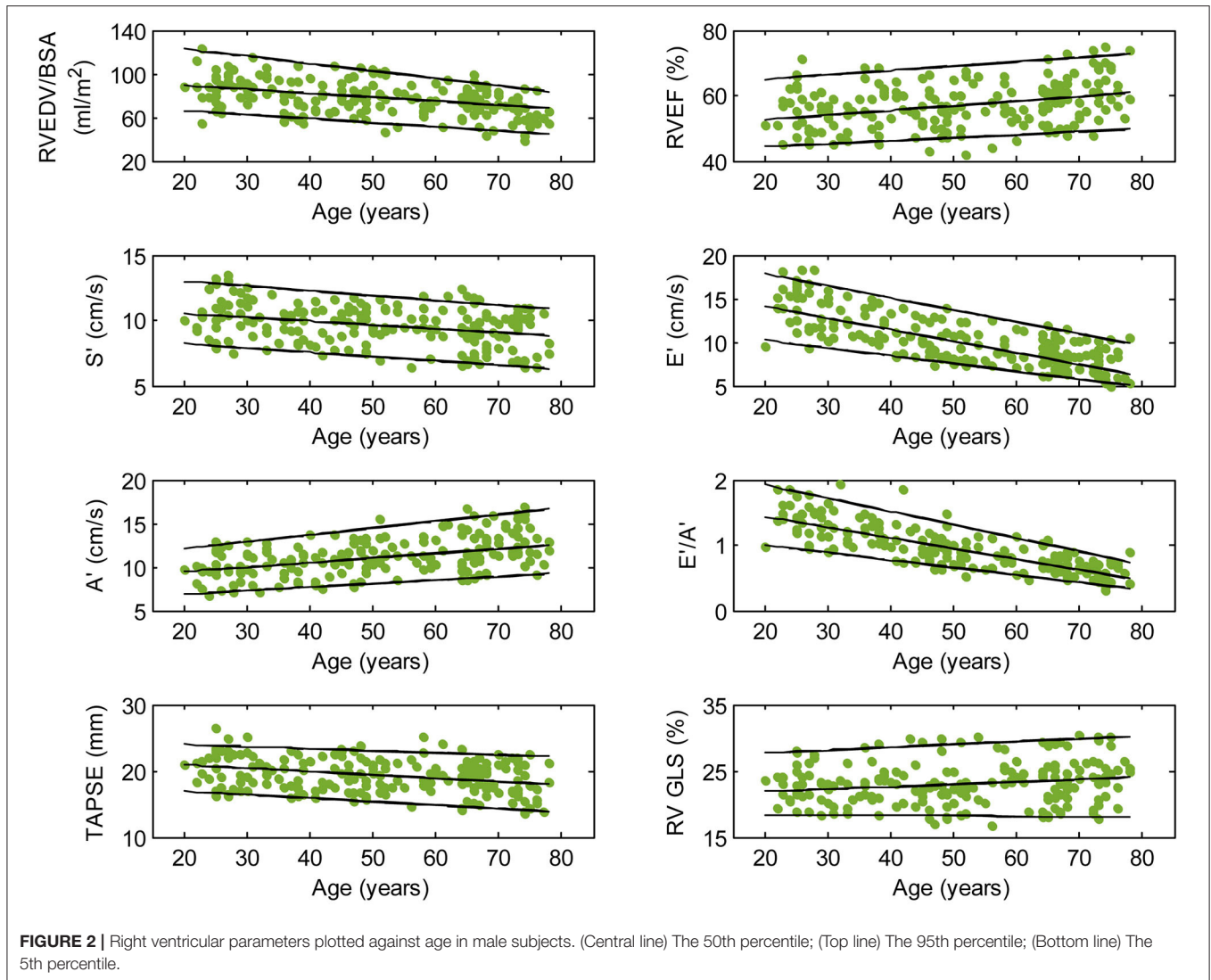
Influence of Sex and Age on Right Ventricular Function

Among RV systolic functional parameters, RVEF and RV GLS were significantly higher in females than in males but there were no significant sex differences in S′, TAPSE, and RV GLSR$_s$ (**Table 1**). RVEF correlated positively with age in both males ($r = 0.31$, $P < 0.0001$) and females ($r = 0.30$, $P < 0.0001$). S′ and TAPSE exhibited negative correlations with age in both males (S′: $r = -0.36$, $P < 0.0001$; TAPSE: $r = -0.28$, $P < 0.0001$) and females (S′: $r = -0.30$, $P < 0.0001$; TAPSE: $r = -0.31$, $P < 0.0001$). RV GLS and RV GLSR$_s$ were not associated with age in both sexes (**Figures 2**, **3**).

With respect to RV diastolic function, females had significantly lower A′ and higher E′/A′ ratios and RV GLSR$_e$ compared to males, but no significant sex differences in E′ and RV GLSR$_a$ were observed (**Table 1**). Among male subjects, E′ ($r = -0.75$, $P < 0.0001$), E′/A′ ratio ($r = -0.80$, $P < 0.0001$) and RV GLSR$_e$ ($r = -0.58$, $P < 0.0001$) decreased significantly with age, whereas A′ ($r = 0.49$, $P < 0.0001$) and RV GLSR$_a$ ($r = 0.57$, $P < 0.0001$) increased with age. Similar positive associations of E′, E′/A′, and RV GLSR$_e$, and negative associations of A′ and RV GLSR$_a$ with age were observed among females (all $P < 0.0001$) (**Figures 2**, **3**).

Influence of Sex and Age on Right Atrial Phasic Function

Females had higher RA reservoir strain, conduit strain, reservoir strain rate, and conduit strain rate compared to males, while RA booster strain and strain rate were similar (**Table 1**). RA reservoir

FIGURE 2 | Right ventricular parameters plotted against age in male subjects. (Central line) The 50th percentile; (Top line) The 95th percentile; (Bottom line) The 5th percentile.

strain, conduit strain, and strain rate correlated negatively with age among both males (reservoir strain: $r = -0.26$, $P < 0.0001$; conduit strain: $r = -0.61$, $P < 0.0001$; conduit strain rate: $r = -0.70$, $P < 0.0001$) and females (reservoir strain: $r = -0.38$, $P < 0.0001$; conduit strain: $r = -0.70$, $P < 0.0001$; conduit strain rate: $r = -0.75$, $P < 0.0001$). Booster strain and strain rate exhibited positive correlations with age among both males (booster strain: $r = 0.46$, $P < 0.0001$; booster strain rate: $r = 0.42$, $P < 0.0001$) and females (booster strain: $r = 0.51$, $P < 0.0001$; booster strain rate: $r = 0.34$, $P < 0.0001$) (**Figures 4**, **5**).
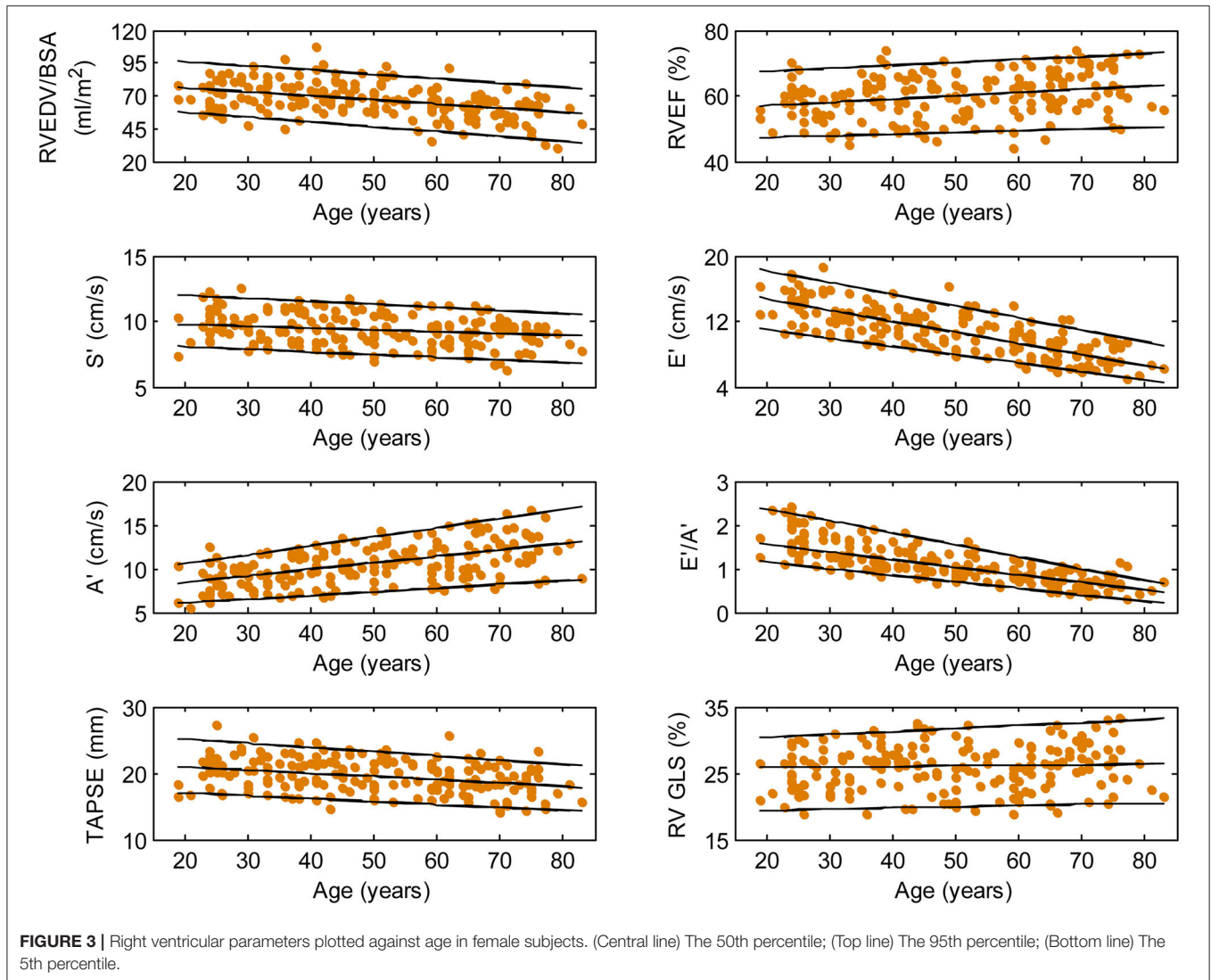
Influence of Sex and Age on Right Ventricular Dimensions

Absolute and indexed RV EDV, ESV, and SV were higher in males compared to females ($P < 0.0001$ for all). Males had larger absolute RV basal and mid-cavity diameters than females (both $P < 0.0001$) but not when normalized to BSA (**Supplementary Table 1**). RV volumes correlated negatively with age among both males (EDV: $r = -0.50$, $P < 0.0001$; ESV: $r = -0.49$, $P < 0.0001$) and females (EDV: $r = -0.39$, $P < 0.0001$; ESV: $r = -0.41$, $P < 0.0001$), with similar correlations after normalization to BSA (males, EDV/BSA: $r = -0.43$, $P < 0.0001$; ESV/BSA: $r = -0.44$, $P < 0.0001$; females, EDV/BSA: $r = -0.45$, $P < 0.0001$; ESV/BSA: $r = -0.44$, $P < 0.0001$). Absolute and indexed RV basal and mid-cavity diameters were not significantly associated with age in both sexes.

Influence of Sex and Age on Right Atrial Dimensions

Males had larger absolute RA diameters and areas compared to females. After normalization to BSA, indexed RA longitudinal and transverse diameters were significantly smaller in males compared to females, while the indexed RA area was not significantly different (**Supplementary Table 1**). Among male subjects, age was positively correlated with indexed RA longitudinal diameter ($r = 0.32$, $P < 0.0001$). Among female

FIGURE 3 | Right ventricular parameters plotted against age in female subjects. (Central line) The 50th percentile; (Top line) The 95th percentile; (Bottom line) The 5th percentile.

subjects, age was positively correlated with indexed RA longitudinal diameter ($r = 0.37$, $P < 0.0001$) and indexed RA area ($r = 0.30$, $P < 0.0001$).

Reproducibility

Good to excellent intra- and inter-observer reproducibility was observed for RV and RA dimensions and volumes, TA velocities and displacement, RV longitudinal strain and strain rates, and RA phasic strains and strain rates (**Table 4**).
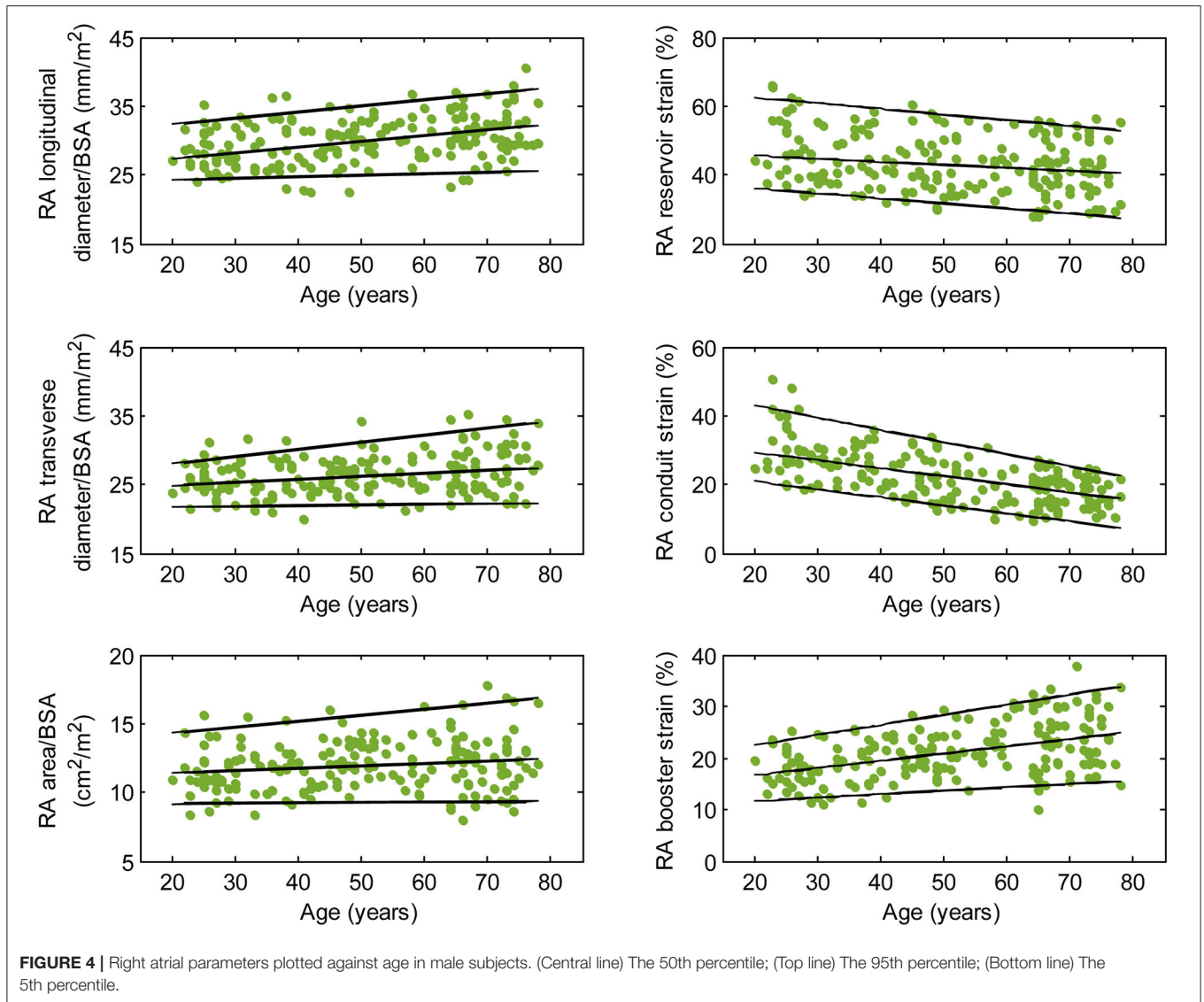
DISCUSSION

In this study, we investigated age- and sex-specific changes in CMR-based right heart dimensions and functional measurements in a large, healthy Asian population. Increased age was associated with impairment of S′ and E′ velocities, TAPSE, and RV GLSR$_e$ and increases in A′ velocity and RV GLSR$_a$, in both sexes. RV GLS and RV GLSR$_s$ were not affected by age in both sexes. As age increased, RA reservoir and conduit strains

and strain rates decreased, while RA booster strain and strain rate increased.

CMR is recommended for many patients at the time of the transition from pediatric to adult congenital heart disease programmes, and this is the gold standard for RV volume, EF, flow quantification, and assessment of extracardiac anatomy. Additionally, CMR is recommended in the presence of clinical deterioration, non-diagnostic echo findings, and prior to surgical or transcatheter intervention [20]. Data on age and sex-specific CMR reference ranges for right heart function in an Asian population are lacking at present. This information is crucial to CMR clinical practice in Asia. Moreover, our CMR-based method is simple, reproducible, and easily implemented for efficient RA and RV function assessment.

This work is novel for a number of reasons. First, it comprises the largest Asian CMR cohort reported to date, enrolling participants from multiple centers to provide broad generalizability of results and high precision in sample estimates of mean and SD. Second, CMR parameters were stratified not

FIGURE 4 | Right atrial parameters plotted against age in male subjects. (Central line) The 50th percentile; (Top line) The 95th percentile; (Bottom line) The 5th percentile.

only by sex but also by age categories across a broad age range of 21–79 years. The increased granularity of results is key to clinical implementation and interpretation in light of the sex- and age-related differences observed in many of the studied parameters. Third, this study is the first to report age- and sex-specific reference ranges for various recently published fast CMR feature tracking parameters used to assess RV systolic and diastolic function as well as phasic RA function.
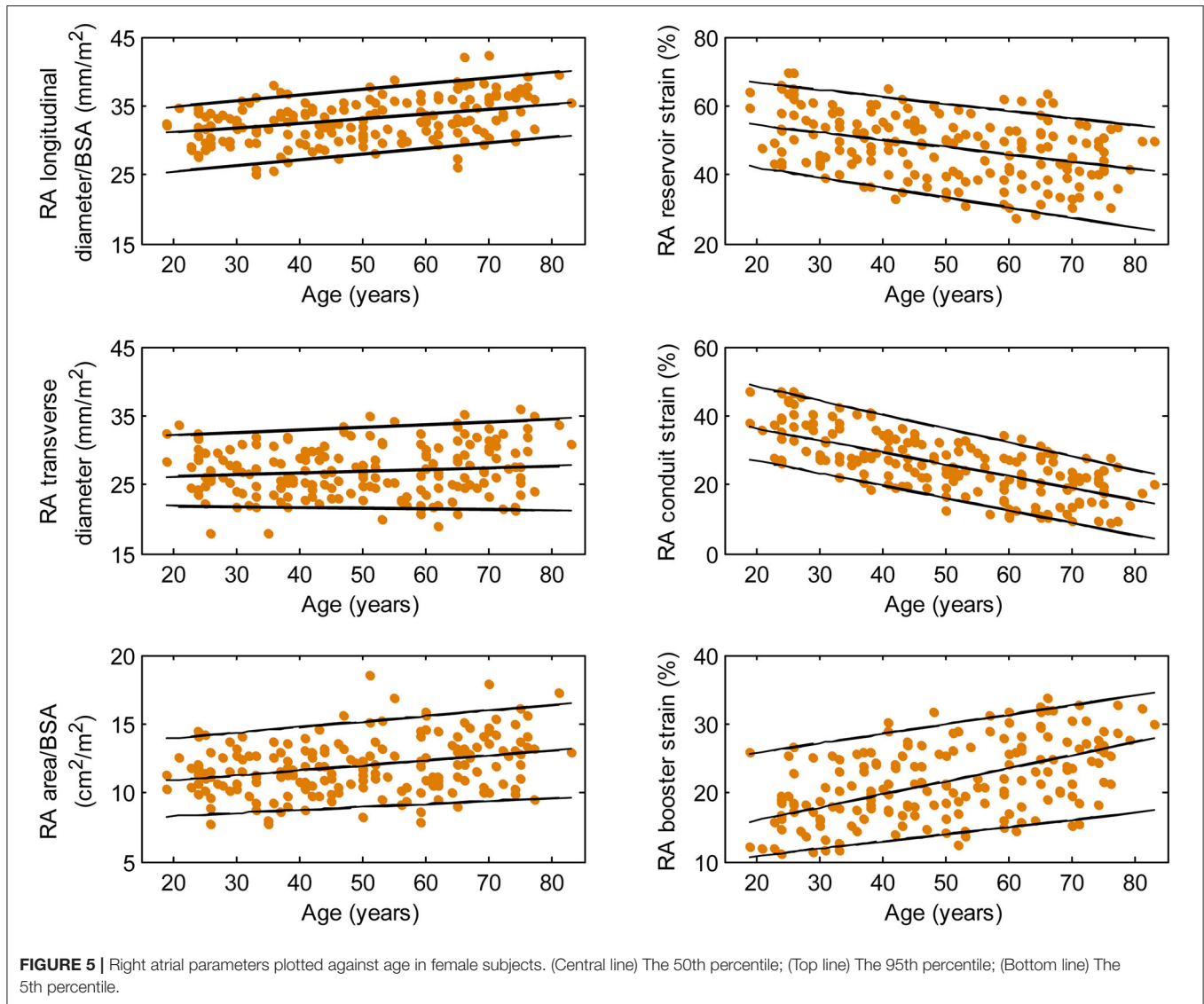
RV Functional Parameters
Asian subjects in our study have numerically smaller right heart size compared to Caucasians in another study (21) (RVEDV: 121 ± 34 vs. 154 ± 40 ml; indexed RVEDV: 72 ± 15 vs. 85 ± 17 ml/m^2), which underscores the need for ethnic-specific reference values. Our study showed a negative correlation between RV volume and age and a positive correlation between RVEF and age, corroborating similar observations in Caucasian subjects (21). Beyond conventional RV volumes and EF, we quantitated

TA dynamics and RV longitudinal strain and strain rates—measurements for assessing RV function in both systole and diastole—and reported their age- and sex-specific reference ranges. Increasing age was associated with reductions in TAPSE, S′, E′, E′/A′, and RV GLSR$_e$ and increases in A′ and RV GLSR$_a$ in both sexes. These results agree with prior studies involving echocardiographic TDI (22) and conventional feature tracking CMR with endocardial contour tracing (23). Of note, we found that RV GLS and RV GLSR$_s$ were not associated with age, which suggests that they are suited to be applied clinically as markers of disease progression unaffected by chronological aging. Our study replicated prior findings of higher systolic functional performance in females than in males as determined by RVEF (21) and RV GLS (24).

RA Functional Parameters
We previously demonstrated that RA function as assessed using our fast RA feature tracking method had important diagnostic

FIGURE 5 | Right atrial parameters plotted against age in female subjects. (Central line) The 50th percentile; (Top line) The 95th percentile; (Bottom line) The 5th percentile.

and prognostic implications in patients with PAH (7). RA volume and function (i.e., emptying fraction) assessment using volumetric analysis requires additional cine CMR acquisitions of atrial short-axis images and post-acquisitional analysis, which are not routinely performed. The area-length method, through geometric assumptions, shortens analysis time slightly (calculation still has to be repeated at all time phases) but is dogged by accuracy and reproducibility issues (25). In our study, we characterized the RA reservoir, conduit, and booster pump functions using strain and strain rate parameters that can be reproducibly and expeditiously measured. These parameters have been shown to be useful for detecting RA dysfunction, RV decompensation, and monitoring disease progression in patients with PAH (7). Among the healthy subjects in our study, females had higher reservoir and conduit strains but similar booster strain compared to males. This is concordant with a previous study of Caucasian subjects (25). In addition, we found age-related changes in RA function manifested as

a significant decrease in conduit strain and an increase in booster strain. We surmise the latter is necessary in order to maintain reservoir strain, which increased slightly with age. These results are in agreement with previous reports using speckle tracking echocardiography (26) and feature tracking CMR with endocardial contour tracing (27).

Advantages of Fast CMR Feature Tracking Parameters

This is the first study to establish age- and sex-specific reference ranges for CMR-derived TA dynamic parameters, which are a prerequisite for clinical applicability and adoption. The CMR-derived TA velocities correlated significantly with TDI-derived measurements, with no angle dependence and excellent reproducibility. This corroborates our previous work which demonstrated good correlation and agreement between CMR-derived mitral annular velocities and TDI measurements (18).

TABLE 4 | Intra- and inter-observer reproducibility for right heart dimension and function parameters.

Parameters	Intra-observer ($n = 20$)		Inter-observer ($n = 20$)	
	Bias (limits of agreement)	CV, %	Bias (limits of agreement)	CV, %
Right ventricular dimension				
RV basal diameter (mm)	0.1 (−1,7, 1.9)	1.6	−2.1 (−4.4, 0.2)	4.4
RV mid-cavity diameter (mm)	1.3 (−0.1, 2.6)	2.7	1.3 (−0.6, 3.2)	3.0
RVEDV (ml)	0.9 (−11.4, 13.2)	3.5	1.4 (−11.6, 14.5)	3.8
RVESV (ml)	−0.3 (−10.8, 10.2)	7.6	2.6 (−8.0, 13.2)	8.9
RVSV (ml)	1.3 (−7.4, 10.0)	4.2	−1.1 (−10.8, 8.6)	4.5
Right atrial dimension				
RA longitudinal diameter (mm)	−0.8 (−2.5, 0.9)	1.5	0.7 (−1.1, 2.6)	1.6
RA transverse diameter (mm)	−0.1 (−4.8, 4.7)	3.6	2.7 (−0.2, 5.5)	4.8
RA area (cm^2)	0.1 (−1.0, 1.1)	1.9	1.2 (−0.5, 2.9)	5.2
Right ventricular function (systolic and diastolic)				
RVEF (%)	0.6 (−6.7, 7.9)	4.2	−1.7 (−9.1, 5.7)	4.5
S′ (cm/s)	−0.1 (−0.9, 0.7)	3.0	−0.2 (−1.3, 1.0)	4.4
E′ (cm/s)	−0.5 (−1.4, 0.5)	4.7	−0.5 (−2.0, 1.0)	6.6
A′ (cm/s)	−0.5 (−2.5, 1.5)	6.6	0.1 (−1.9, 2.0)	5.8
E′/A′	0.1 (−0.2, 0.3)	6.9	−0.1 (−0.3, 0.2)	10.3
TAPSE (mm)	0.1 (−1.2, 1.3)	2.3	0.1 (−1.0, 1.2)	2.1
RV GLS (%)	−0.1 (−1.5, 1.3)	1.9	−0.1 (−2.1, 1.9)	2.7
RV GLSR$_s$ (1/s)	−0.02 (−0.16, 0.11)	3.9	−0.02 (−0.15, 0.10)	3.6
RV GLSR$_e$ (1/s)	−0.01 (−0.24, 0.21)	4.5	−0.04 (−0.34, 0.25)	6.1
RV GLSR$_a$ (1/s)	−0.03 (−0.20, 0.15)	5.5	−0.03 (−0.29, 0.24)	7.9
Right atrial phasic function				
ε_s (%)	0.3 (−2.9, 3.5)	2.9	0.9 (−4.2, 5.9)	4.7
ε_e (%)	0.4 (−2.5, 3.4)	5.5	0.3 (−3.5, 4.1)	6.8
ε_a (%)	−0.1 (−2.5, 2.4)	4.4	0.3 (−2.5, 3.2)	5.3
SR$_s$ (1/s)	0.01 (−0.24, 0.26)	4.0	0.03 (−0.28, 0.33)	5.3
SR$_e$ (1/s)	0.01 (−0.26, 0.27)	5.3	0.02 (−0.28, 0.32)	6.0
SR$_a$ (1/s)	0.06 (−0.27, 0.39)	4.6	−0.03 (-0.38, 0.32)	4.8

CV, coefficient of variation; RV, right ventricular; EDV, end-diastolic volume; ESV, end-systolic volume; SV, stroke volume; EF, ejection fraction; RA, right atrial; S′, peak systolic tricuspid annular velocity; E′, peak early diastolic tricuspid annular velocity; A′, peak late diastolic tricuspid annular velocity; TAPSE, tricuspid annular plane systolic excursion; GLS, global longitudinal strain; GLSR$_s$, peak systolic global longitudinal strain rate; GLSR$_e$, peak early diastolic global longitudinal strain rate; GLSR$_a$, peak late diastolic global longitudinal strain rate; ε_s, right atrial reservoir strain; ε_e, right atrial conduit strain; ε_a, right atrial booster strain; SR$_s$, right atrial reservoir strain rate; SR$_e$, right atrial conduit strain rate; SR$_a$, right atrial booster strain rate.

In addition to TA dynamics, we presented simplified strain indices relating time-varying distances between TA medial and lateral points and a fixed anatomical point at the RV apex or RA roof. Good correlation between the simplified longitudinal strains and those obtained from conventional endocardial contour-based feature tracking CMR was demonstrated, which is consistent with the results of our prior studies involving patients with rTOF, PAH, and age- and sex-matched controls (7, 8). In fact, the accuracy of conventional endocardial feature tracking-derived longitudinal strain is degraded in subjects with vigorous TA motion, as contour tracking of the RV free wall segment adjacent to the tricuspid valve in the long-axis view becomes adversely affected (28). Compared to conventional contour-based strain measurements, the fast feature tracking strain measurements presented in this study are less dependent on RV and RA geometry, and more closely approximate the motion and reflect the function of longitudinal fibers in the RV, which are the greatest contributors to RV contraction (29). Our prior studies have shown that the simplified approach is not only faster but also more reproducible compared to the conventional CMR feature tracking approach (7, 8, 15, 16).

Limitations

There were some limitations in the present study. First, as CMR examinations were not performed repeatedly on the same subjects over time, the associations between age and CMR parameters are cross-sectional, not longitudinal. Nonetheless, the cross-sectional study design is commonly used in studies to establish reference ranges and make inferences regarding relationships in support of further research and clinical studies. We need a longitudinal study with repeated CMR scans on the same individual, which can help us investigate how age affects the heart structural and functional changes. Second, RV mass was not assessed in this study as RV mass is usually not quantified in a routine assessment because of the thin RV myocardium in healthy subjects.

CONCLUSIONS

We investigated age- and sex-related CMR measurements for right heart dimensions and function in a large Asian cohort that are of significant clinical and research utility in Asia. Using CMR, knowledge of age-, sex-, and ethnicity-specific distributions of right heart measurements should aid in the correct interpretation of disease states.

DATA AVAILABILITY STATEMENT

The original contributions presented in the study are included in the article/**Supplementary Materials**, further inquiries can be directed to the corresponding authors.

ETHICS STATEMENT

The studies involving human participants were reviewed and approved by SingHealth Centralized Institutional Review Board. The patients/participants provided their written informed consent to participate in this study.

AUTHOR CONTRIBUTIONS

R-ST, PC, LT, MF, CO, WR, AK, TT, JY, JT, YC, and LZ conceived the study design. SL, JG, CG, and XZ analyzed data. SL, R-ST, PC, LT, MF, CO, WR, AK, TT, JY, JT, YC, and LZ interpreted results. JA performed statistical analysis. SL drafted manuscript.

JG, R-ST, PC, LT, MF, CG, XZ, CO, JA, WR, AK, TT, JY, JT, YC, and LZ edited and revised manuscript. All authors read and approved the final manuscript.

SUPPLEMENTARY MATERIAL

The Supplementary Material for this article can be found online at: https://www.frontiersin.org/articles/10.3389/fcvm.2021.664431/full#supplementary-material

REFERENCES

1. Sanz J, Sánchez-Quintana D, Bossone E, Bogaard HJ, Naeije R. Anatomy, function, and dysfunction of the right ventricle: JACC state-of-the-art review. *J Am Coll Cardiol.* (2019) 73:1463–82. doi: 10.1016/j.jacc.2018.12.076

2. Geva T. Is MRI the preferred method for evaluating right ventricular size and function in patients with congenital heart disease? MRI is the preferred method for evaluating right ventricular size and function in patients with congenital heart disease. *Circ Cardiovasc Imaging.* (2014) 7:190–7. doi: 10.1161/CIRCIMAGING.113.000553

3. Schulz-Menger J, Bluemke DA, Bremerich J, Flamm SD, Fogel MA, Friedrich MG, et al. Standardized image interpretation and post processing in cardiovascular magnetic resonance: Society for Cardiovascular Magnetic Resonance (SCMR) Board of Trustees Task Force on Standardized Post Processing. *J Cardiovasc Magn Reson.* (2013) 15:35. doi: 10.1186/1532-429X-15-35

4. Leng S, Jiang M, Zhao XD, Allen JC, Kassab GS, Ouyang RZ, et al. Three-dimensional tricuspid annular motion analysis from cardiac magnetic resonance feature-tracking. *Ann Biomed Eng.* (2016) 44:3522–38. doi: 10.1007/s10439-016-1695-2

5. Ito S, McElhinney DB, Adams R, Bhatla P, Chung S, Axel L. Preliminary assessment of tricuspid valve annular velocity parameters by cardiac magnetic resonance imaging in adults with a volume-overloaded right ventricle: comparison of unrepaired atrial septal defect and repaired tetralogy of Fallot. *Pediatr Cardiol.* (2015) 36:1294–300. doi: 10.1007/s00246-015-1160-2

6. Maffessanti F, Gripari P, Pontone G, Andreini D, Bertella E, Mushtaq S, et al. Three-dimensional dynamic assessment of tricuspid and mitral annuli using cardiovascular magnetic resonance. *Eur Heart J Cardiovasc Imaging.* (2013) 14:986–95. doi: 10.1093/ehjci/jet004

7. Leng S, Dong Y, Wu Y, Zhao XD, Ruan W, Zhang GC, et al. Impaired CMR-derived rapid semi-automated right atrial longitudinal strain is associated with decompensated hemodynamics in pulmonary arterial hypertension. *Circ Cardiovasc Imaging.* (2019) 12:e008582. doi: 10.1161/CIRCIMAGING.118.008582

8. Leng S, Tan RS, Guo JJ, Chai P, Zhang GC, Teo L, et al. Cardiovascular magnetic resonance-assessed fast global longitudinal strain parameters add diagnostic and prognostic insights in right ventricular volume and pressure loading disease conditions. *J Cardiovasc Magn Reson.* (2021) 23:38. doi: 10.1186/s12968-021-00724-5

9. De Siqueira MEM, Pozo E, Fernandes VR, Sengupta PP, Modesto K, Gupta SS, et al. Characterization and clinical significance of right ventricular mechanics in pulmonary hypertension evaluated with cardiovascular magnetic resonance feature tracking. *J Cardiovasc Magn Reson.* (2016) 18:39. doi: 10.1186/s12968-016-0258-x

10. Xie E, Yu R, Ambale-Venkatesh B, Bakhshi H, Heckbert SR, Soliman EZ, et al. Association of right atrial structure with incident atrial fibrillation: a longitudinal cohort cardiovascular magnetic resonance study from the Multi-Ethnic Study of Atherosclerosis (MESA). *J Cardiovasc Magn Reson.* (2020) 22:36. doi: 10.1186/s12968-020-00631-1

11. Kawut SM, Lima JA, Barr RG, Chahal H, Jain A, Tandri H, et al. Sex and race differences in right ventricular structure and function: the multi-ethnic study of atherosclerosis-right ventricle study. *Circulation.* (2011) 123:2542–51. doi: 10.1161/CIRCULATIONAHA.110.985515

12. Koh AS, Gao F, Leng S, Kovalik JP, Zhao XD, Tan RS, et al. Dissecting clinical and metabolomics associations of left atrial phasic function by cardiac magnetic resonance feature tracking. *Sci Rep.* (2018) 8:8138. doi: 10.1038/s41598-018-26456-8

13. Valsangiacomo Buechel ER, Mertens LL. Imaging the right heart: the use of integrated multimodality imaging. *Eur Heart J.* (2012) 33:949–60. doi: 10.1093/eurheartj/ehr490

14. Maceira AM, Cosín-Sales J, Roughton M, Prasad SK, Pennell DJ. Reference right atrial dimensions and volume estimation by steady state free precession cardiovascular magnetic resonance. *J Cardiovasc Magn Reson.* (2013) 15:29. doi: 10.1186/1532-429X-15-29

15. Leng S, Tan RS, Zhao XD, Allen JC, Koh AS, Zhong L. Fast long-axis strain: a simple, automatic approach for assessing left ventricular longitudinal function with cine cardiovascular magnetic resonance. *Eur Radiol.* (2020) 30:3672–83. doi: 10.1007/s00330-020-06744-6

16. Leng S, Tan RS, Zhao XD, Allen JC, Koh AS, Zhong L. Validation of a rapid semi-automated method to assess left atrial longitudinal phasic strains on cine cardiovascular magnetic resonance imaging. *J Cardiovasc Magn Reson.* (2018) 20:71. doi: 10.1186/s12968-018-0496-1

17. Leng S, Ge H, He J, Kong LC, Yang YN, Yan FH, et al. Long-term prognostic value of cardiac MRI left atrial strain in ST-segment elevation myocardial infarction. *Radiology.* (2020) 296:299-309. doi: 10.1148/radiol.2020200176

18. Leng S, Zhao XD, Huang FQ, Wong JI, Su BY, Allen JC, et al. Automated quantitative assessment of cardiovascular magnetic resonance-derived atrioventricular junction velocities. *Am J Physiol Heart Circ Physiol.* (2015) 309:H1923–35. doi: 10.1152/ajpheart.00284.2015

19. Ouyang RZ, Leng S, Sun AM, Wang Q, Hu LW, Zhao XD, et al. Detection of persistent systolic and diastolic abnormalities in asymptomatic pediatric repaired tetralogy of Fallot patients with preserved ejection fraction: a CMR feature tracking study. *Eur Radiol.* (2021). doi: 10.1007/s00330-020-07643-6

20. Di Salvo G, Miller O, Babu Narayan S, Li W, Budts W, Valsangiacomo Buechel ER, et al. Imaging the adult with congenital heart disease: a multimodality imaging approach-position paper from the EACVI. *Eur Heart J Cardiovasc Imaging.* (2018) 19:1077–98. doi: 10.1093/ehjci/jey102

21. Petersen SE, Aung N, Sanghvi MM, Zemrak F, Fung K, Paiva JM, et al. Reference ranges for cardiac structure and function using cardiovascular magnetic resonance (CMR) in Caucasians from the UK Biobank population cohort. *J Cardiovasc Magn Reson.* (2017) 19:18. doi: 10.1186/s12968-017-0327-9

22. Dalen H, Thorstensen A, Vatten LJ, Aase SA, Stoylen A. Reference values and distribution of conventional echocardiographic Doppler measures and longitudinal tissue Doppler velocities in a population free from cardiovascular disease. *Circ Cardiovasc Imaging.* (2010) 3:614–22. doi: 10.1161/CIRCIMAGING.109.926022

23. Peng JP, Zhao XD, Zhao L, Fan ZM, Wang Z, Chen H, et al. Normal values of myocardial deformation assessed by cardiovascular magnetic resonance feature tracking in a healthy Chinese population: a multicenter study. *Front Physiol.* (2018) 9:1181. doi: 10.3389/fphys.2018.01181

24. Qu YY, Li H, Rottbauer W, Ma GS, Buckert D, Rasche V. Right ventricular free wall longitudinal strain and strain rate quantification with cardiovascular magnetic resonance based tissue tracking. *Int J Cardiovasc Imaging.* (2020) 36:1985–96. doi: 10.1007/s10554-020-01895-5

25. Maceira AM, Cosin-Sales J, Prasad SK, Pennell DJ. Characterization of left and right atrial function in healthy volunteers by cardiovascular magnetic resonance. *J Cardiovasc Magn Reson.* (2016) 18:64. doi: 10.1186/s12968-016-0284-8

26. Peluso D, Badano LP, Muraru D, Dal Bianco L, Cucchini U, Kocabay G, et al. Right atrial size and function assessed with three-dimensional and speckle-tracking echocardiography in 200 healthy volunteers. *Eur Heart J Cardiovasc Imaging.* (2013) 14:1106–14. doi: 10.1093/ehjci/jet024

27. Truong VT, Palmer C, Young M, Wolking S, Ngo TNM, Sheets B, et al. Right atrial deformation using cardiovascular magnetic resonance myocardial feature tracking compared with two-dimensional speckle tracking echocardiography in healthy volunteers. *Sci Rep.* (2020) 10:5237. doi: 10.1038/s41598-020-62105-9

28. Bhave NM, Visovatti SH, Kulick B, Kolias TJ, McLaughlin VV. Right atrial strain is predictive of clinical outcomes and invasive hemodynamic data in group 1 pulmonary arterial hypertension. *Int J Cardiovasc Imaging.* (2017) 33:847–55. doi: 10.1007/s10554-017-1081-7

29. Brown SB, Raina A, Katz D, Szerlip M, Wiegers SE, Forfia PR. Longitudinal shortening accounts for the majority of right ventricular contraction and improves after pulmonary vasodilator therapy in normal subjects and patients with pulmonary arterial hypertension. *Chest.* (2011) 140:27-33. doi: 10.1378/chest.10-1136